

# A Decision Tree Based Approach Towards Adaptive Profiling of Cloud Applications

Ioannis Giannakopoulos  
Computing Systems  
Laboratory  
School of ECE, NTUA, Greece  
ggiann@cslab.ece.ntua.gr

Dimitrios Tsoumakos  
Department of Informatics  
Ionian University, Corfu,  
Greece  
dtsouma@ionio.gr

Nectarios Koziris  
Computing Systems  
Laboratory  
School of ECE, NTUA, Greece  
nkoziris@cslab.ece.ntua.gr

## ABSTRACT

Cloud computing has allowed applications to allocate and elastically utilize massive amounts of resources of different types, leading to an exponential growth of the applications' configuration space and increased difficulty in predicting their performance. In this work, we describe a novel, automated profiling methodology that makes no assumptions on application structure. Our approach utilizes oblique Decision Trees in order to recursively partition an application's configuration space in disjoint regions, choose a set of representative samples from each subregion according to a defined policy and returns a model for the entire configuration space as a composition of linear models over each subregion. An extensive experimental evaluation over real-life applications and synthetic performance functions showcases that our scheme outperforms other state-of-the-art profiling methodologies. It particularly excels at reflecting abnormalities and discontinuities of the performance function, allowing the user to influence the sampling policy based on the modeling accuracy, the space coverage and the deployment cost.

## 1. INTRODUCTION

Performance modeling is a well-researched problem in traditional computing [28, 45, 29]. The identification of an application's behavior under different configurations is a key factor for it to be able to fulfill its objectives. Since the advent of the Cloud era, an increasing number of applications has been migrated to the cloud [35]: Reduced administrative costs, allocation of near-infinite resources in a pay-as-you-go manner, increased availability, etc. are some of the merits of deploying over the Cloud. Nevertheless, cloud infrastructures add extra layers of complexity to the modeling problem due to virtualization (virtual CPUs, disks, network interfaces, etc.) and the shared nature of the resource pools (oversubscription and colocation). At the same time, new opportunities for application deployments have emerged: Any application can be instantly deployed in numerous ways, allocating different types of resources and in different quantities so as to maximize its performance in a cost-effective way. The configuration space of the application has been vastly expanded, making the problem of creating a performance model considerably harder. Lack of such a model, also called an *application profile*, could lead to suboptimal cloud deployments, performance degradations, decreased revenue and reduced availability. Moreover, since cloud providers frame their infrastructures over highly heterogeneous software and hardware resources (e.g., different

CPU architectures, storage backends, networking configurations), an application profile is bound with these resources since a given application may not behave identically over different environments.

Given the above, an automated estimation of a cloud application profile would prove highly beneficial. The magnitude of the configuration space makes all exhaustive approaches that demand the exploration of the entirety (or at least a large part) of the configuration space impractical, since they entail both a prohibitive number of cloud deployments and an enormous amount of computation. Several approaches target to model cloud offerings [11] and application performance [19, 50, 34, 38] in an analytical way. These approaches are effective for known applications with specific structure and are based on simulation or emulation techniques [37, 25]. To overcome the rigidity of these schemes, several methods [23, 22, 30, 31] take a "black-box" approach, in which the application receives a set of inputs, corresponding to the different factors of the configuration space and produces one or more outputs, corresponding to the achieved performance. These approaches try to identify the relationship between the input and the output variables for a subset of the configuration space (utilizing sampling) and generalize the findings with Machine Learning techniques (modeling). The types of sampling and modeling techniques utilized are of key importance for the effectiveness of these approaches. Regarding sampling, the application must be deployed for a set of representative configurations so as to effectively capture its behavior. For the modeling part, the appropriate classification approaches must be chosen, taking into consideration the nature of the profiling data.

In this work, we propose an approach to automatically generate an application profile for any application deployed over a cloud infrastructure given a specific number of deployments. Our work tackles the sampling and modeling steps in a unified way. First, we introduce an accuracy-driven sampling technique that favors regions of the configuration space which are not accurately approximated. Second, we decompose the configuration space in disjoint regions and utilize different models to approximate the application performance for each of them. The basis of our methodology lies on the theory of Classification and Regression Trees [10]. CARTs showcase a set of interesting properties that make them an excellent candidate for our methodology: They are easy to implement, scalable to multiple dimensions, robust, suitable both for nominal and categorical attributes and natively function in a "divide-and-conquer" manner that fits our formulation. By utilizing an augmented version of CART, we

manage to recursively partition the configuration space of the application into disjoint regions. Each partition is assigned with a number of configurations to be deployed. The process is iterated until a pre-defined maximum number of sample configurations is reached. The number of configurations spent at each region is adaptively decided according to a number of parameters such as the approximation error, the size of each partition and the monetary cost of the configuration. Finally, the entire space is approximated by linear models per partition, based on the deployed configurations. Intuitively, our approach attempts to “zoom-in” to regions where application performance is not accurately approximated, paying specific interest to all the abnormalities and discontinuities of the performance function. By utilizing oblique Decision Trees [9], we are able to capture patterns that are affected by multiple configuration parameters simultaneously. This property is particularly useful to identify performance bottlenecks, peaks and other interesting patterns in the application’s behavior. In summary, we make the following contributions:

(a) We propose an adaptive, accuracy-driven profiling technique for applications deployed over cloud environments that utilizes oblique Decision Trees. Our method natively decomposes the multi-dimensional input space into disjoint regions, naturally adapting to the complex performance application behavior in a fully automated manner. Our scheme utilizes three unique features relative to the standard Decision Tree algorithm: First, it proposes a novel expansion algorithm that constructs oblique Decision Trees by examining whether the obtained samples fit into a linear model. Second, it allows developers to providing a compromise between *exploring* the configuration space and *exploiting* the previously obtained knowledge. Third, it adaptively selects the most accurate profiling model, based on the achieved accuracy.

(b) We perform an extensive experimental evaluation over diverse, real-world applications and synthetic performance functions of various complexities. Our results showcase that our methodology is the most efficient, achieving modeling accuracies even  $3\times$  higher than its competitors and, at the same time, it is able to create models that reflect abnormalities and discontinuities of the performance function orders of magnitude more accurately. Furthermore, it is interesting to note that our sampling methodology proves to be particularly beneficial for linear classifiers and ensembles of them, as linear models trained with samples chosen by our scheme present even 38% lower modeling error. Lastly, we showcase how our scheme can easily include other parameters in its policy, respecting monetary costs besides the modeling error and the size of the configuration space.

## 2. BACKGROUND

First, we provide a mathematical formulation of the problem of creating a performance model. We provide all the necessary definitions and notations and, next, a brief overview of the Decision Tree theory.

### 2.1 Problem formulation

The problem of creating a performance model for a cloud application can be formulated as a classic function approximation problem [14, 22]. The application is viewed as a black-box that receives a number of inputs and produces a single (or more) output(s). The main idea behind construct-

ing the performance model is to predict the relationship between the inputs and the output, without making any assumption regarding the application’s architecture. In other words, one would want to identify a function that projects the input variables into the output for every possible input value. Inputs reflect any parameters able to affect the application performance: Different types of resources (e.g., number of cores, amount of memory, number of nodes for horizontally scalable applications, etc.), application-level parameters (e.g., amount of cache used by an RDBMS, HDFS block size, replication factor, etc.), workload-specific parameters (e.g., throughput and type of requests) and dataset-specific parameters (e.g., size, location, distribution, etc.) are the most representative categories of such inputs.

Assume that an application comprises  $n$  inputs and a single output. We assume that the  $i^{th}$  input,  $1 \leq i \leq n$ , may receive values from a predefined finite set of values, denoted as  $d_i$ . The Cartesian product of all  $d_i, 1 \leq i \leq n$  is referred to as the *Deployment Space* of the application  $D = d_1 \times d_2 \times \dots \times d_n$ . Essentially, the Deployment Space contains all possible combinations of values for each application input. Similarly, the output of the application produces values that correspond to a performance metric, indicative of the application’s ability to fulfill its objectives. The set of the application’s output will be referred to as the *Performance Space* of the application  $P$ . Based on the definitions of  $D$  and  $P$ , we define the performance model  $m$  of an application as a function mapping points from  $D$  to  $P$ , i.e.,  $m : D \rightarrow P$ . The estimation of the performance model of an application entails the estimation of the performance value  $b_i \in P$  for each  $a_i \in D$ . However,  $|D|$  increases exponentially with  $n$  (since  $|D| = \prod_{i=1}^n |d_i|$ ), thus the identification of all the performance values becomes impractical, both in terms of computation and budget. A common approach to address this challenge is the extraction of a subset  $D_s \subseteq D$ , much smaller than the original Deployment Space and the estimation of the performance points  $P_s$  for each  $a_i \in D_s$ . Using  $D_s$  and  $P_s$ , model  $m$  can be approximated, creating an approximate model denoted as  $m'$ . The difference between  $m$  and  $m'$  is indicative of the accuracy of the later: the shorter the difference, the more accurate the approximate model becomes. The accuracy of  $m'$  is greatly influenced by two factors: (a) the set  $D_s$  and (b) the modeling method used to create  $m'$ .

The methodology introduced in this work addresses both factors in a unified way. Specifically, we employ a Decision Tree-based method to recursively partition the Deployment Space into smaller regions into which the performance function appears to have similar behavior. This mechanism is utilized both for modeling and the identification of  $D_s$ . Decision Trees are based on the idea of dividing the space into disjoint regions and address each region separately. This “divide-and-conquer” approach fits naturally into this problem, since cloud applications tend to present behavioral patterns in disjoint regions of their deployment spaces [20, 15]. Specifically, the typical behavior of an horizontally scalable application is to increase its performance when more resources are utilized, up to a point after which it remains intact. For example, in [20] this is demonstrated for three popular NoSQL databases for various performance metrics and different types of resources whereas in [15] the same behavior is also depicted for Hadoop and MongoDB.

Finally, it should be emphasized that the application pro-

finding problem resembles the *Global Optimization* problem, in which the optimal configuration for an application in order to achieve the highest performance is explored. The two problems, although sharing similar formulations, as both view the applications as black-boxes, greatly differ in the following: The later formulation seeks for an optimal point, whereas the former seeks for a suitable *set* of representative points in order to construct an accurate model. To this end, the techniques utilized for solving optimization problems such as Gradient Descent, Simulated Annealing, etc., cannot be applied on the problem addressed by this work due to its combinatorial nature. On the contrary, we exploit Decision Trees for the identification of this representative subset  $D_s \subseteq D$ , as discussed in the following section.

## 2.2 Decision Trees

*Classification and Regression Trees (CART)* [10], or Decision Trees, are a very popular classification and regression approach. They are formed as tree structures containing a set of intermediate nodes, also called *test* nodes, and a set of *leaf* nodes. Each test node represents a boundary of the space of the data and each leaf node represents a class, if the Decision Tree is used for classification, or a linear model, if it is used for regression. The boundaries of the Decision Tree divide the original space into a set of disjoint regions.

The construction of a Decision Tree is based on recursively partitioning the space of the data so as to create disjoint groups of points that maximize their intra-group homogeneity and minimize their inter-group homogeneity. The metric for expressing the homogeneity of a group differs among the existing algorithms. *GINI impurity* has been used by the CART algorithm [10], whereas *Information Gain* has been used by ID3 [40] and C4.5 [39]. These metrics are only used when the Decision Tree is used for classification. When used for regression, the Variance Reduction metric is used [10]. In the classic form of the Decision Trees, the aforementioned heuristics are applied on each leaf to decide which dimension should be used for partitioning and at which value. The usage of these metrics does not lead to an optimal tree though, since it is proven that the construction of an optimally sized Decision Tree is an NP-complete problem [27]. The termination condition for the construction varies between different algorithms: In many cases, the tree length is pre-defined whereas in other cases the termination condition is dictated by its accuracy (if the expansion of the tree marginally benefits its accuracy, the construction algorithm stops).

Each boundary of a Decision Tree is parallel to one axis of the data, since it only involves a single dimension of the data space (the boundary line is expressed by a rule of the form  $x_i = c$ , where  $c$  is a constant value). If we generalize this rule into a multi-variate line, then we obtain the *oblique* Decision Trees [9] formed from lines which are no longer axis-parallel and each test node retains a boundary that can be expressed by a line of the form:  $\sum_{i=1}^n c_i x_i + \gamma = 0$ . To better illustrate this, in Figure 1 we provide an example where we showcase the tree structure along with the respective partitions of the Deployment Space for a tree that has 3 leaves and 2 test nodes. The original (or *flat*) Decision Trees can be considered as a special case of the oblique Decision Trees. The multivariate boundaries boost the expressiveness of the Decision Tree, since non axis-parallel patterns can be recognized and expressed. However, the estimation of a multivariate boundary line is much more complex than

the estimation of a flat line, since it entails the calculation of combinations of values among all the different dimensions. As a compromise, a simple solution has been introduced [48]: Estimating the multivariate line that only involves the two most important dimensions. Important dimensions are considered those that offer the highest intra-group homogeneity (measured with one of the heuristics presented before), if they were selected as a single variate boundary. The selection of those dimensions occurs in each leaf *separately*, in the sense that different leaves can select different dimensions as the most important ones.

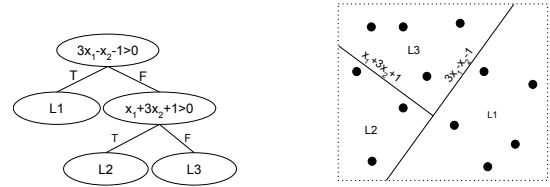


Figure 1: Example of an Oblique Decision Tree

In this paper, we are utilizing oblique Decision Trees in two ways: First, we are employing them to create an approximate model of the performance function. Second, we are exploiting their construction algorithm to adaptively sample the Deployment Space of the application, focusing more on regions where the application presents a complex behavior and ignoring regions where its behavior tends to be predictable. These uses are extensively described in Sections 3.2 and 3.3 respectively. Essentially, Decision Trees allow us to “zoom in” to regions of the Deployment Space and create partitions in such a manner that a linear hyperplane can successfully represent the data points within the respective region. To further enhance their capabilities, we introduce a new heuristic for the expansion of the leaf nodes, representing whether samples within a region can be accurately expressed by a linear hyperplane.

## 2.3 Method overview

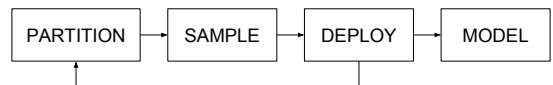


Figure 2: Method overview

Before proceeding to the presentation of the profiling algorithm, let us provide a high level overview of our methodology. The main idea of the suggested algorithm is to partition the Deployment Space of the application by grouping samples that better fit different linear models, obtain knowledge about the performance function through sampling the Deployment Space, deploying the selected configurations and, when a predefined number of deployments has been reached, model the performance function utilizing different linear models for each partition. This is schematically represented in Figure 2.

Specifically, at each step, the Deployment Space is partitioned into the shortest possible regions by grouping the already obtained samples according to their ability to create a linear model that accurately approximates the application

performance; Estimates are then created regarding the intra-group homogeneity. The homogeneity of each region corresponds to the accuracy of the prediction of the performance function for the specified region. Therefore, less accurate regions must be further sampled to clarify the behavior of the performance function in them. On the contrary, more accurate regions are considered successfully approximated, thus new samples need not be obtained for those. Conceptually, the suggested algorithm is an attempt to adaptively “zoom-in” to areas of the Deployment Space where the behavior of the performance function is more *obscure*, in the sense that it is unpredictable and hard to model. This enables the number of allowed application deployments to be elastically distributed inside the Deployment Space, leading to more accurate predictions as more samples are collected for performance areas that are harder to approximate. The properties of Decision Trees, heavily utilized throughout this work, render them a perfect candidate for our approach: Their ease of implementation, scalability, robustness and, especially, their divide-and-conquer functionality, that allows for adaptiveness in focusing on the regions of unpredictable application performance, are some of those. All these properties inherently fit the application profiling problem and allow us to decompose the complex Deployment Spaces into simpler subspaces and address different regions with different models.

### 3. PROFILING METHODOLOGY

In this section we provide an extensive description of the profiling methodology. For readability reasons, we decompose the core functionalities into separate functions, which are discussed in the following sections.

#### 3.1 Algorithm Overview

**Algorithm 1** DT-based Adaptive Profiling Algorithm

---

```

1: procedure DTADAPTIVE( $D, B, b$ )
2:    $tree \leftarrow \text{TREEINIT}(\emptyset), samples \leftarrow \emptyset$ 
3:   while  $|samples| \leq B$  do
4:      $tree \leftarrow \text{EXPANDTREE}(tree, samples)$ 
5:      $s \leftarrow \text{SAMPLE}(D, tree, samples, b)$ 
6:      $d \leftarrow \text{DEPLOY}(s)$ 
7:      $samples \leftarrow samples \cup d$ 
8:    $model \leftarrow \text{CREATEMODEL}(samples)$ 
9:   return  $model$ 

```

---

Our Algorithm takes three input parameters: (a) the Deployment Space of the application  $D$ , (b) the maximum number of application deployments  $B$  and (c) the number of deployments triggered at each iteration of the algorithm  $b$ . The  $tree$  variable represents a Decision Tree, while the  $samples$  set contains the obtained samples. While the number of obtained samples has not reached  $B$ , the following steps are executed: First, the leaves of the tree are examined and tested whether they can be replaced by subtrees that further partition their regions (Line 4). Next, the leaves of the expanded tree are sampled according to the  $SAMPLE$  function (Line 5), and the chosen samples are deployed (Line 6) according to the deployment configuration of the sample, and performance metrics are obtained. One must note the difference between  $s$  and  $d$ :  $s \subseteq D$  whereas  $d \subseteq D \times P$ , where  $D$  and  $P$  are the Deployment and Performance space respec-

tively, as defined in Section 2.1.  $s$  members are points of the Deployment Space representing a deployment configuration, whereas  $d$  members represent a point of the performance function that *contains* the respective input space point plus the performance value. Finally, when  $B$  samples have been chosen, the final model is created (Line 8).

Before presenting each function in more detail, some observations can be made regarding the algorithm’s execution. First, the tree is incrementally expanded at each iteration and its height is gradually increased. The arrival of new samples leads to the formulation of new rules for partitioning the Deployment Space (represented by test nodes in the tree structure), leading to an *online* training scheme. Second, the  $DEPLOY$  function (Line 6) is responsible for making  $|s|$  deployments of the application according to the configuration setups specified by each  $s_i \in s$  and return the same configuration points accompanied by their performance metric. This implies that  $|s| = |d|$  and this is the most time consuming part of each iteration, since resource orchestration for most cloud providers requires several minutes. Lastly, the total number of iterations is equal to  $\lceil \frac{B}{b} \rceil$ .

#### 3.2 Decision Tree Expansion

The expansion of a Decision Tree is equivalent to turning its leaves into subtrees consisting of test nodes and new leaf nodes. This transformation creates new partitions in the regions of the Deployment Space represented by the leaves. Let us recall here that any leaf node of a Decision Tree contains sets of sample points. These sample points depict Deployment Space points along with their respective performance values. Furthermore, each leaf represents a specific region of the Deployment Space. To identify the exact boundaries of a leaf, one would traverse the tree upwards (from the leaf up to the root) to compose the boundary lines represented by the test nodes of the tree. If those boundaries are multivariate, i.e., the Decision Tree is oblique, the represented region will not be axis-parallel. Figure 3 shows the top view of a two dimensional Deployment Space. The samples (depicted as black dots) consist of three dimensions:  $x_1$  (horizontal axis),  $x_2$  (vertical axis) and a performance dimension that is perpendicular to the surface of the Figure and is not shown. We now provide the algorithm that estimates a new boundary line for a given leaf (Algorithm 2).

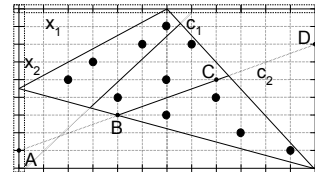


**Figure 3:** Example leaf of an oblique DT

The algorithm receives three input parameters: the set of sample points in the leaf and two lists of values that retain all possible values of the two most important dimensions for the specified region (these values are highlighted with a dotted line in Figure 3). If the samples consist of more than two dimensions, the two most important dimensions are chosen using the methodology presented in Section 2.2, where we choose the dimensions that would create the most homogeneous regions/leaves if axis-parallel cuts were to be created. First, we estimate a regression model for all the

samples and evaluate its accuracy using Cross Validation [21] (Lines 2-3). Next, we create a set of two dimensional points (*points*) that correspond to all combinations of the values contained in  $u_1, u_2$  (Lines 4-7). Graphically, these points lie on the grid generated when we draw axis-parallel lines from each value of  $u_1, u_2$ . As seen in Figure 3, these points may not necessarily lie within the region of the leaf.

---

**Algorithm 2** Partitioning function

---

```

1: procedure SPLITLEAF(samples,  $u_1$ ,  $u_2$ )
2:    $uModel \leftarrow$  regression(samples)
3:    $error \leftarrow$  crossValidation( $uModel$ , samples)
4:    $points \leftarrow \square$ 
5:   for  $t_1 \in u_1$  do
6:     for  $t_2 \in u_2$  do
7:        $points \leftarrow points \cup (t_1, t_2)$ 
8:    $bestLine, examinedL \leftarrow \emptyset$ 
9:   for  $p_1 \in points$  do
10:    for  $p_2 \in points$  and  $p_1 \neq p_2$  do
11:       $splitLine \leftarrow$  estimateLine( $p_1$ ,  $p_2$ )
12:      if  $splitLine \notin examinedL$  then
13:         $examinedL \leftarrow examinedL \cup splitLine$ 
14:         $lSam, rSam \leftarrow \emptyset$ 
15:        for  $s \in samples$  do
16:          if  $s \preceq splitLine$  then
17:             $lSam \leftarrow lSam \cup s$ 
18:          else
19:             $rSam \leftarrow rSam \cup s$ 
20:           $lModel \leftarrow$  regression( $lSam$ )
21:           $rModel \leftarrow$  regression( $rSam$ )
22:           $lErr \leftarrow$  crossValidation( $lModel$ ,  $lSam$ )
23:           $rErr \leftarrow$  crossValidation( $rModel$ ,  $rSam$ )
24:           $avgErr \leftarrow \frac{|lSam| \cdot lErr + |rSam| \cdot rErr}{|lSam| + |rSam|}$ 
25:           $minError \leftarrow \infty$ 
26:          if ( $avgErr \leq c_o \cdot error$ ) then
27:            if ( $avgErr \leq minError$ ) then
28:               $bestLine \leftarrow splitLine$ 
29:               $minError \leftarrow avgErr$ 
30:   return  $bestLine$ 

```

---

Subsequently, the algorithm, examines all possible combinations of points, creating candidate split lines that will be used to partition the leaf. Line 11 represents the estimation of such a split line, based on the two dimensional points  $p_1$  and  $p_2$ . Since different couples of points may create the same lines (e.g., points  $A, B, C, D$  from Figure 3) we keep log of the lines that have been examined so far to avoid recalculation. Two disjoint sets of samples are then created by partitioning the original *samples* set, using the candidate split line (Line 16-19). In Line 16, the symbol  $\preceq$  is used to describe the relationship between the position of the point relative to the split line. Specifically, assume that  $s$ 's coordinates for dimensions referred to by  $x_1$  and  $x_2$  are  $(x_1^s, x_2^s)$  and the split line is  $x_2 = ax_1 + b$ . We say that  $s \preceq splitLine$  if and only if  $x_2^s \leq ax_1^s + b$ .

After the partitioning is completed, two regression models are trained for the two disjoint subsets of samples and the respective cross validation error of these models is calculated and averaged (Lines 20-23). This computationally expensive approach was preferred against the Variance Reduction heuristic due to its increased performance, as demonstrated in Appendix C.3. The best split line is the one that pro-

duces the lowest error with the condition that this error is less than a constant value  $c_o$ ,  $0 < c_o \leq 1$  times the error of the original model. This threshold is set to avoid overfitting, i.e., the model starts to describe the noise of the training data and the generalisation of the model becomes less accurate. The value of  $c_o$  is experimentally set. In our evaluation we set it equal to 0.95. To clarify the expansion methodology, we provide an example in Figure 4, in which Algorithm 2 is executed over the tree depicted in Figure 1. In this example, nodes L1 and L3 have been substituted with the subtrees containing the leaf nodes  $L4-L5$  and  $L6-L7$  respectively. One may notice here that node  $L2$  was not further partitioned since it does not contain enough samples. Node  $L1$  was replaced by a test node representing an axis parallel boundary. This process is applied on every leaf node of the Decision Tree until no leaves can be further expanded.

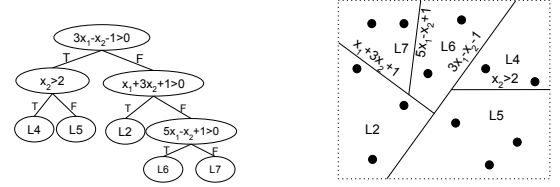


Figure 4: Expansion of an Oblique Decision Tree

### 3.3 Sampling

After the tree is expanded, the *SAMPLE* function is executed (Algorithm 3).

---

**Algorithm 3** Sampling algorithm

---

```

1: procedure SAMPLE( $D$ , tree, samples,  $b$ )
2:    $errors, sizes \leftarrow \emptyset$ ,  $maxError, maxSize \leftarrow 0$ 
3:   for  $l \in leaves(tree)$  do
4:      $points \leftarrow \{d | d \in samples, d.in \in l\}$ 
5:      $m \leftarrow$  regression(points)
6:      $errors[l] \leftarrow$  crossValidation( $m, points$ )
7:      $sizes[l] \leftarrow |\{e \in D \cap l\}|$ 
8:     if  $maxError \leq errors[l]$  then
9:        $maxError \leftarrow errors[l]$ 
10:    if  $maxSize \leq sizes[l]$  then
11:       $maxSize \leftarrow sizes[l]$ 
12:    $scores, newSamples \leftarrow \emptyset$ ,  $sumScores \leftarrow 0$ 
13:   for  $l \in leaves(tree)$  do
14:      $scores[l] \leftarrow w_{error} \cdot \frac{errors[l]}{maxError} + w_{size} \cdot \frac{sizes[l]}{maxSize}$ 
15:      $sumScores \leftarrow sumScores + scores[l]$ 
16:   for  $l \in leaves(tree)$  do
17:      $leafNoDeps \leftarrow \lceil \frac{scores[l]}{sumScores} \cdot b \rceil$ 
18:      $s \leftarrow$  RANDOMSELECT( $\{d | d \in D \cap l\}$ ,  $leafNoDeps$ )
19:      $newSamples \leftarrow newSamples \cup s$ 
20:   return  $newSamples$ 

```

---

After the initialization of the necessary variables (Line 2), the algorithm iterates over the leaves of the tree (Line 3). For each leaf, the samples are filtered and those that belong inside the specified leaf are kept. This is demonstrated in Line 4, where *d.in* indicates the dimensions of sample *d* that refer to the Deployment Space. A regression model is then created, based on the filtered points and its error accuracy is calculated (Lines 5-6). Again, the Cross Validation

methodology is utilized for the error estimation. The size of the specified leaf is then estimated. The size is equal to the number of acceptable deployment combinations, i.e., the points of the Deployment Space lying inside the region of the specified leaf. Thus, the portion of the Deployment Space that is represented by the leaf is an estimate of its size. Different estimates could also be used (e.g., measuring the surface of the leaf). This representation was chosen due to its simplicity. One must note the difference between the sets  $\{d|d \in \text{samples}, d.in \in l\}$  (Line 4) and  $\{e|e \in D \cap l\}$  (Line 7): The former refers to the already deployed samples and its members consist of  $|D|+|P|$  dimensions, whereas the later consists of Deployment Space points of  $|D|$  dimensions. Finally, after storing both the error and the size of each leaf into a dictionary, the maximum leaf error and size are calculated (Lines 8-11). Subsequently, a score is estimated for each leaf (Lines 13-15). The score of each leaf is set to be proportional to its scaled size and error. This normalization is executed so as to guarantee that the impact of the two factors is equivalent. Two coefficients  $w_{error}$  and  $w_{size}$  are used to assign different weights to each measure. These scores are accumulated and used to proportionally distribute  $b$  to each leaf (Lines 16-19). In that loop, the number of deployments of the specified leaf is calculated and new samples from the subregion of the Deployment Space are randomly drawn with the *RANDOMSELECT* function, in a uniform manner. Finally, the new samples set, containing samples from all the leaves, is returned.

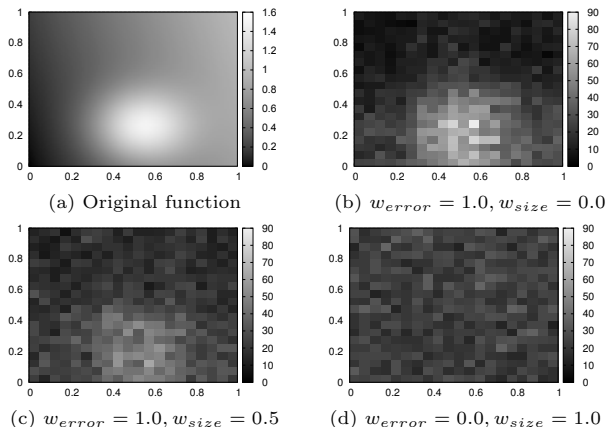


Figure 5: Sample distribution for different weights

To further clarify the sampler’s functionality, we provide an example of execution for a known performance function of the form  $y = 0.8 \cdot x_1 + 0.2 \cdot x_2$ . On a randomly selected point, we introduced an abnormality modeled by a Gaussian function. In Figure 5 (a) we provide a projection of the performance function. The horizontal and vertical axes represent  $x_1$  and  $x_2$  respectively and the colors represent the values of  $y$ , where the lighter colors demonstrate higher  $y$  values. We execute Algorithm 1 and alter the values of  $w_{error}$ ,  $w_{size}$  during the sampling step. We assume a maximum number of deployments  $B$  of 100 points out of the 2500 available points and a per-iteration number of deployments  $b$  of 10 points. In Figures 5 (b), (c) and (d) we provide the distribution of the selected samples, for different weight values. Each dimension is divided in 20 intervals and for each execution we keep count of the samples that appear inside

each region. The color of the regions demonstrate the number of the samples within the region (lighter colors imply more samples). In Figure (b) the score of each leaf is only determined by its error. Most samples are gathered around the Gaussian distribution: The first leaves that represent the area of the Gaussian function produce less accurate models since they cannot express the performance function with a linear model. Since the score of each leaf is only determined by its error, these leaves claim the largest share of  $b$  at each step, thus the samples are gathered around the abnormality. On the contrary, when increasing  $w_{size}$  as in Figure (c), the gathering of the samples around the abnormality is neutralized as more samples are now distributed along the entire space, something that is intensified when  $w_{error} = 0$  and  $w_{size} > 0$  in Figure (d) where the abnormality can no longer be detected just by examining the samples’ distribution.

The consideration of two factors (error and size) for deciding the number of deployments spent at each leaf targets to solve the trade-off of assigning samples for *exploring* the Deployment Space versus *exploiting* the obtained knowledge, i.e., focus on the abnormalities of the space and allocate more points to further examine them. This is a well-known trade-off in many fields of study [46]. In our approach, one can favor either direction by adjusting the weights of leaf error and size, respectively. Taking this one step further, using a score function allows us to take multiple parameters into consideration. For cloud-based applications, the deployment cost is one such criterion. Deployment coordinates are not equally costly as providers charge for specific resources. For example, VMs with more cores or main memory may cost more. In order to profile an application taking into consideration the monetary cost as well, we could assume a score function of the following form,  $l$  being the specified leaf:

$$score(l) = w_{error} \cdot error(l) + w_{size} \cdot size(l) - w_{cost} \cdot cost(l) \quad (1)$$

in which the cost of the leaf is calculated as the average cost of the deployment points inside the leaf. Such a function would penalize leaves that contain more expensive deployment configurations. Adjusting the way each factor affects the scoring function allows developers to achieve a satisfactory compromise between the contradicting parameters of focusing on the most unpredictable regions (through error), exploring the space (through size) and minimizing the monetary cost of profiling the application (through cost).

### 3.4 Modeling and performance optimizations

After  $B$  samples have been returned by the profiling algorithm, the samples are then given as input to the *CRE-ATEMODEL* (Algorithm 1, Line 8) function so as to train a new Decision Tree. The choice of training a new Decision Tree instead of expanding the one used during the sampling phase of the algorithm was made to maximize the accuracy of the final model by creating more accurate partitions on the higher levels of the tree. When the first test nodes of the former Decision Tree were created, only a short portion of the samples were available to the profiling algorithm and, hence, it is possible that this Decision Tree may have created inaccurate partitions. To tackle this limitation, the final set of samples is used to train the final model from scratch. However, in cases where the number of obtained samples is comparable to the dimensionality of the Deployment Space, Decision Trees suffer from the following

deficiency: The number of constructed leaves is extremely short and, hence, the tree degenerates into a linear regression model that covers sizeable regions of the deployment space. Taking into consideration that various performance functions may present strongly non-linear characteristics, the accuracy of the end model could degrade. To tackle this problem, along with the Decision Tree we also train a set of Machine Learning classifiers and keep the one that achieves the lowest Cross Validation error. From our evaluation, we have determined that for lower sampling rates alternative classifiers such as Multi-Layer Perceptrons [43] and Ensembles of Classifiers [16] (with Perceptrons as base classifier) may achieve higher accuracy. When the Decision Tree is trained with enough samples, it can achieve an accuracy that outperforms all the other classifiers. This is the main reason for choosing the Decision Tree as a base model for our scheme: The ability to provide higher expressiveness by composing multiple linear models in areas of higher unpredictability, make them a perfect choice for modeling the performance of cloud based applications.

The aforementioned deficiency, in which the tree is poorly partitioned in the first algorithm iterations, can also produce vulnerabilities for the sampling step. Specifically, it can create a pathological case where the Deployment Space is erroneously partitioned on the first levels of the tree and then, as new samples arrive, more deployments are spent on creating more and shorter regions that, could otherwise have been merged into a single leaf. This is a typical problem when a Decision Tree is created in an “online” fashion. To tackle this challenge, several solutions have been proposed [47]. In our approach, we introduce the step of recreating the Decision Tree from scratch prior to the sampling step. This optimization, albeit requiring extra computation, boosts the performance of the profiling methodology as better partitioning of the space leads to more representative regions and better positioned models, as indicated by our evaluation provided in Appendix C. Nevertheless, the time needed for this extra computation is marginal when compared to the time needed to deploy the application during the deployment step (Algorithm 1, Line 6) that might require several minutes, according to the application and the executed workload.

### 3.5 Complexity analysis

The most time-consuming step of our methodology is the tree expansion step (Algorithm 1, Line 4). Specifically, for each leaf, the algorithm requires:

$$\mathcal{O}((|u_1| \cdot |u_2|)^2 \cdot n^2 \cdot |samples|)$$

steps ( $u_1, u_2$  being the value lists as expressed in Algorithm 2,  $n$  being the dimensionality of the Deployment Space and  $|samples|$  is the total number of samples), since the most time consuming part of the for loops (Algorithm 2 Lines 9–10) is the estimation of the linear model (Algorithm 2, Lines 22–23). This estimation is done for  $|points|^2$  times, where  $|points| = |u_1| \cdot |u_2|$ , and its complexity is equal to  $\mathcal{O}(n^2 \cdot |samples|)$ , hence the above complexity. To further simplify the above expression, we can replace the cardinality of  $u_1, u_2$  with the highest dimension cardinality, say  $k$ . Since  $|samples| = B$ , the total complexity of the *SPLITLEAF* function is equal to:  $\mathcal{O}(k^4 n^2 B)$ . *SPLITLEAF* is invoked for each leaf, the number of which is proportional to  $B$ , thus,

the complexity of each iteration is equal to:

$$\mathcal{O}(k^4 n^2 B^2)$$

This complexity may look prohibitive, however, Algorithm 1 is executed “offline”. The *DEPLOY* function (Line 6) dominates the execution time of the profiling algorithm in general, thus such a high complexity is marginal against the time needed to deploy the application and execute the selected workload.

## 4. EVALUATION

In this section, we provide the experimental evaluation of our methodology. First, we evaluate the performance of our scheme (Algorithm 1) against other end-to-end profiling approaches. We then provide a thorough analysis of the different parameters that impact the algorithm’s performance.

### 4.1 Methodology and data

To evaluate the accuracy of our profiling algorithm, we test it over various real and synthetic performance functions. We are using the *Mean Squared Error* (MSE) and *Mean Absolute Error* (MAE) metrics for the comparison, estimated over the *entire* Deployment Space, i.e., we exhaustively deployed all the possible combinations of each application’s configurations, so as to ensure that the generated model successfully approximates the original function for the entire space. We have deployed four different popular real-world applications, summarized in Table 1. Specifically, two batch applications from the HiBench [26] benchmark used for data analytics and two interactive applications have been selected: The Media Streaming application from the cloudsuite [18] benchmark and a data serving benchmark (MongoDB) from PerfKitBenchmarker [6]. Our objective was to select representative, complex as well as popular applications from the three benchmark suites. Several applications were omitted from our evaluation due to their non-distributed architecture (e.g., the data caching and web service benchmarks from [18]) or their resemblance with the selected applications (e.g., aerospike, cassandra benchmarks from [6]). Our evaluation is mainly focused on the sampling and modeling parts of profiling, ignoring the deployment time. In Appendix A, we provide a detailed analysis of the deployment process, along with an estimate of the deployment time for all the tested applications.

Table 1: Applications table

Application (perf. metric)	Dimension	Values
Spark Bayes (execution time)	YARN nodes	4–20
	# cores per node	2–8
	memory per node	2–8 GB
	# of documents	0.5–2.5 ( $\times 10^6$ )
Hadoop Wordcount (execution time)	# of classes	50–200 classes
	YARN nodes	2–20
	# cores per node	2–8
	memory per node	2–8 GB
Media Streaming (throughput)	dataset size	5–50 GB
	# of servers	1–10
	video quality	144p–1440p
MongoDB (throughput)	request rate	50–500 req/s
	# of MongoDB	2–10
MongoS (throughput)	# of MongoS	2–10
	request rate	5–75 ( $\times 10^3$ ) req/s

The first two applications (Bayes and Wordcount) are deployed on a YARN [49] cluster. YARN creates the abstraction of a unified resource pool in terms of memory and cores. New tasks claim an amount of resources which are either provided to them (and the task is executed) or, if not available, stall until the resources become available. The Media Streaming application consists of two components: The backend is an NFS server that provides the videos to the Web Servers. A number of lightweight Web Servers (nginx) are setup to serve the videos to the clients. The NFS server retains 7 different video qualities and 20 different videos per quality. For simplicity, we assume that the possible workloads will only request videos from a specific quality, i.e., two users may not, in parallel, request videos of different qualities. Finally, MongoDB is deployed as a sharded cluster and it is queried using YCSB [13]. The sharded deployment of MongoDB consists of three components: (a) a configuration server that holds the cluster metadata, (b) a set of nodes that store the data (represented as MongoD) and (c) a set of loadbalancers that act as endpoints to the clients (represented as MongoS). Since MongoD and MongoS components are single-threaded, we only consider the cases of scaling them horizontally. Each of the aforementioned applications was deployed in a private Openstack installation, with 8 nodes aggregating 200 cores and 600G of RAM. In Appendix B we provide a detailed analysis of the chosen applications and showcase the impact of each input dimension to their performance.

**Table 2: Synthetic performance functions**

Complexity	Name	Function	$R^2$
LOW	LIN	$f_1(\mathbf{x}) = a_1x_1 + \dots + a_nx_n$	1.00
	POLY	$f_2(\mathbf{x}) = a_1x_1^2 + \dots + a_nx_n^2$	0.95
AVERAGE	EXP	$f_3(\mathbf{x}) = e^{f_1(\mathbf{x})}$	0.65
	EXPABS	$f_4(\mathbf{x}) = e^{ f_1(\mathbf{x}) }$	0.62
	EXPSQ	$f_5(\mathbf{x}) = e^{-f_1(\mathbf{x})^2}$	0.54
HIGH	GAUSS	$f_6(\mathbf{x}) = e^{-f_2(\mathbf{x})}$	0.00
	WAVE	$f_7(\mathbf{x}) = \cos(f_1(\mathbf{x})) \cdot f_3(\mathbf{x})$	0.00
	HAT	$f_8(\mathbf{x}) = f_2(\mathbf{x}) \cdot f_6(\mathbf{x})$	0.00

We have also generated a set of performance functions using mathematical expressions. The functions are listed in Table 2. Each function maps the Deployment Space to a single dimensional Performance Space and consists of  $n$  dimensions such that  $\mathbf{x} = (x_1, x_2, \dots, x_n)$ . The listed functions were chosen with the intention to test our profiling algorithm against multiple scenarios of varying complexity. To quantify each function’s complexity, an idea would be to measure how accurately a function can be approximated by a linear model. Linear performance functions can be approximated with only a handful of samples, hence we regard them as the least complex case. For each of the listed performance functions, we calculate a linear regression model that best represents the respective data points and test its accuracy using the coefficient of determination  $R^2$ . Values close to 1 indicate that the specified functions tend to linearity, i.e., the linear model can represent them with high accuracy, whereas values close to zero indicate that the specified functions are strongly non-linear. Based on the values of  $R^2$  for each case, we generate three complexity classes: Functions of *LOW* complexity (when  $R^2$  is higher than 0.95), functions of *AVERAGE* complexity (when  $R^2$  is between 0.5 and 0.7) and functions of *HIGH* complexity when  $R^2$  is

close to zero. The values of  $R^2$  depicted in Table 2 refer to two-dimensional Deployment Spaces. In Appendix B, we utilize the same methodology to categorize the complexity of the real-world applications.

## 4.2 Profiling algorithms comparison

First, we compare our profiling methodology against other end-to-end profiling schemes. Our approach is referred to as Decision Tree-based Adaptive methodology (*DTA*). Active Learning [44] (*ACTL*) is a Machine Learning field that specializes on exploring a performance space by obtaining samples assuming that finding the class (if used for classification) or the output value (if used for regression) of the sample is computationally hard. More specifically, we implemented *Uncertainty Sampling* that prioritizes the points of the Deployment Space with the highest uncertainty, i.e., points for which a Machine Learning model cannot predict their class or continuous value with high confidence. Similarly, PANIC [22] is an adaptive approach that favors points belonging into steep areas of the performance function, with the intuition that the abnormalities of the performance function characterize it best. Furthermore, since most profiling approaches use a randomized sampling algorithm [23, 14, 30, 31] to sample the Deployment Space and different Machine Learning models to approximate the performance, we implement a profiling scheme where we draw random samples from the performance functions and approximate them using the models offered by WEKA [24], keeping the most accurate in each case. In all but a few cases, the Random Committee [42] algorithm prevailed, constructed using Multi-Layer Perceptron as a base classifier. We consider a sampler that draws the samples in a Uniform way (*UNI*) and a sampler that while drawing the samples uniformly, also attempts to maximize the coverage of the Deployment Space such as the Latin Hypercube Sampler (*LHS*) [36]. As these two samplers showcase very similar results we only demonstrate *UNI*. For each of the aforementioned methodologies, we execute the experiments 20 times and present the median of the results.

### 4.2.1 Sampling rate

We first compare the four methods against a varying Sampling Rate, i.e., the portion of the Deployment Space utilized for approximating the performance function ( $SR = \frac{|D_s|}{|D|} \times 100\%$ ). SR varies from 3% up to 20% for the four real-world applications. In Figure 6 we provide the accuracy of each approach measured in terms of MSE. In Appendix C.1 we also provide the accuracy expressed in terms of MAE.

From Figure 6, it becomes apparent that *DTA* outperforms all the competitors for increasing Sampling Rates, something indicative of its ability to distribute the available number of deployments accordingly so as to maximize the modeling accuracy. In more detail, all algorithms benefit from an increase in Sampling Rate since the error metrics rapidly degrade. In Bayes, when the sampling rate is around 3% *UNI* and *DTA* construct models of the highest accuracy. As mentioned in Section 3.4, for such low Sampling Rates the linearity of the Decision Tree would fail to accurately represent the relationship between the input and the output dimensions, thus a Random Committee classifier based on Multi-Layer Perceptrons is utilized for the approximation. The same type of classifier also achieves the highest accuracy for the rest of the profiling algorithms (*ACTL*, *PANIC*) that, as seen from the Figure, present higher errors due to

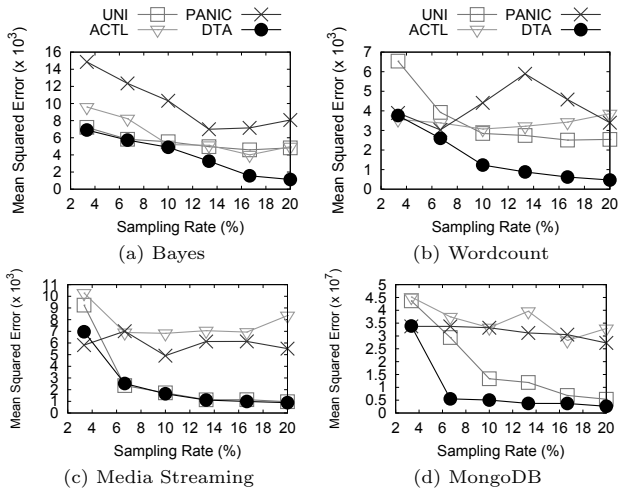


Figure 6: Accuracy vs sampling rate (MSE)

the less accurate sampling policy at low SR. When the Sampling Rate increases, the Decision Tree obtains more samples and creates more leaves, which contributes in the creation of more linear models that capture a shorter region of the Deployment Space and, thus, producing higher accuracy. Specifically, for  $SR > 3\%$ , Decision Tree created a more accurate prediction than other classifiers and, hence, it was preferred.

In the rest of the applications, Wordcount is similar to Bayes, since both are executed over the same engine (Hadoop) and address resources in a similar way. Media Streaming, on the other hand, exhibits an entirely different behavior. The selected dimensions affect the performance almost linearly, thus the produced performance function is smooth and easily modeled by less sophisticated algorithms than DTA. This explains why DTA presents the same performance with UNI. PANIC and ACTL try to identify the abnormalities of the space and fail to produce accurate models. Finally, for the MongoDB case, DTA outperforms the competitors increasingly with SR. In almost all cases, DTA outperforms its competitors and creates models even 3 times more accurate (for Bayes when  $SR = 20\%$ ) from the best competitor. As an endnote, the oscillations in PANIC’s and ACTL’s behavior are explained by the aggressive exploitation policy they implement. PANIC does not explore the Deployment Space and only follows the steep regions, whereas ACTL retains a similar policy only following the regions of uncertainty, hence the final models may become overfitted in some regions and fail to capture most patterns of the performance function. Our work identifies the necessity of spending the available deployments not only for exploring the regions of uncertainty but also for covering the entire space. This compromise between these counterbalancing aspects is unique in DTA and explains the reason for its prevalence.

#### 4.2.2 Performance function complexity

We now compare the accuracy of the profiling algorithms against the complexity of the profiling functions. We create synthetic performance functions from those presented in Table 2. For each of them, we generate two datasets with two and five dimensions, using random coefficients for each dimension and constant Deployment Space size of 10K points. We run the profiling algorithms for each function assuming

sampling rates of 0.5% and 2.0% and present the results in Table 3. Since the output dimension of each dataset is in different scale, we normalize all the results, dividing the error of each methodology with the error produced by UNI. LIN, EXP and EXPSQ were approximated successfully from all methodologies, i.e., the achieved errors were less than  $10^{-5}$  so they are not included in the Table. The scores in bold demonstrate the lowest errors for each case.

Table 3 showcases that *all* synthetic functions were approximated more accurately by DTA than the rest of the profiling algorithms. Specifically, even in the most complex cases (GAUSS, WAVE and HAT), DTA achieves lower errors and the difference between the competitors is increasing with the Sampling Rate. Again, we notice that increasing SR greatly benefit the accuracy of DTA since more samples allow it to focus more on the unpredictable regions of the Deployment Space. Regarding the rest of the profiling methodologies, the attribute of ACTL and PANIC to almost exclusively focus on regions where the performance function presents oscillating behavior leads them to an increasing difference with UNI, especially when the function’s complexity increases and the oscillations become more frequent. On the contrary, it is observed that when the performance functions are characterized totally from their abnormality, i.e., a discontinuity or another pattern appearing in specific regions of the Deployment Space, like in the EXPABS case, both of them create very accurate models. In this case, we observe that DTA produces results of high quality too: For both Sampling Rates it presents results similar to PANIC’s and in the 2% case, DTA marginally outperforms it. DTA manages to outperform all the competitors, even when the performance function is far more complex than an expected cloud application function.

Table 3: Accuracy vs function complexity

	n	ACTL		PANIC		DTA	
		0.5%	2%	0.5%	2%	0.5%	2%
POLY	2	1.03	1.57	1.05	1.23	<b>0.80</b>	<b>0.89</b>
	5	0.99	1.05	0.98	1.22	<b>0.97</b>	<b>0.45</b>
EXPABS	2	8.99	5.29	1.29	2.63	<b>0.18</b>	<b>0.32</b>
	5	0.40	0.91	<b>0.13</b>	0.12	<b>0.13</b>	<b>0.11</b>
GAUSS	2	1.55	5.91	0.92	5.63	<b>0.28</b>	<b>0.42</b>
	5	2.25	5.99	1.86	1.47	<b>0.99</b>	<b>0.67</b>
WAVE	2	0.98	2.34	1.01	2.51	<b>0.91</b>	<b>0.99</b>
	5	1.10	1.13	1.08	1.02	<b>0.97</b>	<b>0.77</b>
HAT	2	1.17	6.49	1.25	4.85	<b>0.60</b>	<b>0.42</b>
	5	8.01	4.77	6.63	4.20	<b>0.99</b>	<b>0.95</b>

To summarize, let us recall that the provided evaluation takes place for the *entire* Deployment Space and not only for abnormal regions. As the complexity of a function increases, the ability of a profiling algorithm to identify the complex regions and isolate them becomes crucial for its accuracy. Using oblique Decision Trees, DTA manages to quickly identify those regions and, as we will see in Section 4.3.2, produce models that accurately reflect them with extremely low error. Furthermore, due to their inherent divide-and-conquer nature, Decision Trees are proven to be particularly efficient for Deployment Spaces of increasing dimensionality as they achieve to decompose the space according to the dimensions’ importance and, as seen by Table 3, retain satisfying accuracy, in contrast to the rest of the approaches.

### 4.3 Parameter Impact Analysis

We now study the parameters that affect DTA’s perfor-

mance. We utilize the Bayes application to showcase our points, since it comprises the most dimensions and can be considered as the most complex among the real ones we tested. For each discussed parameter, we examine its impact on two factors: The accuracy of the algorithm and the execution overhead it imposes, measured in terms of execution time. Each experiment is executed twenty times and the median values are presented.

### 4.3.1 Per-iteration number of deployments

One of the most important parameters in DTA’s execution is  $b$ : This is the number of deployments distributed among the leaves of the tree in each iteration. In Figure 7, we provide results where  $b$  is set as a portion of  $B$ , that is the total number of allowed deployments, for three different sampling rates. The horizontal axis represents the ratio  $\frac{B}{b}$ . The Figure on the left depicts the MSE metric while the right one represents the respective execution time of DTA.

When  $\frac{B}{b} = 1$ , the algorithm degenerates into a random algorithm such as UNI, since the whole tree is constructed in one step. At this point, the algorithm presents the highest error and the lowest execution time, since the tree is only constructed once and the most erroneous leaves are not prioritized. When the ratio increases, the algorithm produces more accurate results and the decrease in error becomes more profound as the Sampling Rate increases. For example, when  $SR = 20\%$  the error decreases 2.5 times while the ratio increases. However, when  $SR = 5\%$  and  $SR = 10\%$  and for low  $b$  values (e.g.,  $1/10$  of  $B$ ) an interesting pattern becomes apparent. In these cases, the error metric starts to increase, neutralizing the effect of low  $b$ . This occurs in cases where  $b$  is extremely small, compared to the dimensionality of the Deployment Space<sup>1</sup>. In such cases,  $b$  at each iteration is harder to be evenly distributed to the leaves. The leaves with the lowest scores are almost always ignored due to rounding  $b$  (since each leaf must be assigned with an integer number of samples). We can conclude that although low  $b$  values have a positive effect into the algorithm’s accuracy, extremely low  $b$  values that make it comparable to the dimensionality of the space tend to compromise its accuracy.

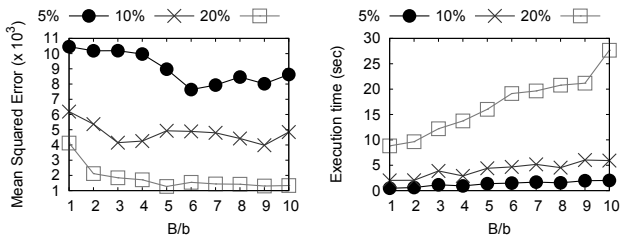


Figure 7: Accuracy vs  $b$

The performance gain observed by increasing  $\frac{B}{b}$  can be attributed to two factors: (a) the final Decision Tree has more accurate cuts and, hence, well-placed models and (b) the samples are properly picked during the profiling. To isolate the impact of these two factors, we repeat the same experiment for all applications and train different ML classifiers instead of a Decision Tree. This way, we isolate the impact

<sup>1</sup>A sampling rate of 5% for the Bayes application is equivalent to approximately 60 Deployment Space points, thus  $b$  is equal to 6 points, which is very close to the dimensionality of the Deployment Space.

of sampling and examine its magnitude. We identified that the classifiers that consist of linear models, i.e., regression classifiers such as OLS (Ordinary Least Squares) [17], or an Ensemble of Classifiers created with Bagging [41] (BAG) that utilize linear models as base improve their accuracy with increasing  $\frac{B}{b}$ . In Table 4 we provide our findings for two classifiers (OLS and BAG) for three of the four applications; Media Streaming is too smooth, as it does not contain abnormalities or discontinuities, and hence a sophisticated sampling algorithm is not essential for the extraction of an accurate profile. In the Table we provide the percentage difference in MSE of each compared to the case  $\frac{B}{b} = 1$ .

The table demonstrates that, for all cases, an increasing  $\frac{B}{b}$  benefits the linear models, something that showcases that our sampling algorithm itself achieves better focus on the interesting Deployment Space regions. Nevertheless, we notice that an increasing  $\frac{B}{b}$  ratio does not always lead to linear error reduction. When  $\frac{B}{b} = 8$  and  $\frac{B}{b} = 10$ , one can notice that the error either degrades marginally (for Bayes) or slightly increases (for MongoDB) when compared to the  $\frac{B}{b} = 5$  case. This is ascribed to the extremely low per-iteration number of deployments  $b$  that, as mentioned before, when  $\frac{B}{b}$  increases,  $b$  becomes comparable to the dimensionality of the Deployment Space and, hence, the proportional distribution of  $b$  according to the leaves’ scores is negatively affected. Other tested classifiers such as Perceptrons or Support Vector Machines remain unaffected by  $\frac{B}{b}$ . Yet, our findings demonstrate that even a mere utilization of the sampling part of our methodology can be particularly useful in cases where linear models, or a composition of them, are required.

Table 4: Error degradation for different classifiers

Applications	Classifier	B/b			
		2	5	8	10
Bayes	OLS	-23%	-27%	-28%	-29%
	BAG	-23%	-22%	-21%	-23%
Wordcount	OLS	-23%	-17%	-19%	-23%
	BAG	-21%	-28%	-41%	-38%
MongoDB	OLS	-19%	-13%	-12%	-7%
	BAG	-6%	-12%	-11%	-2%

### 4.3.2 Oblique boundaries

We now compare the effect of flat versus oblique Decision Trees in the profiling accuracy and execution time. In Figure 8 (a), we provide the results for the Bayes application for various sampling rates.

The oblique tree, i.e., a tree with multi variate test nodes, introduces a slight accuracy gain (of about 10% for low sampling rates) compared to the flat tree, as seen by the left subfigure while, simultaneously, demands about twice the time for algorithm execution. The accuracy gains fade out when the Sampling Rate increases. This phenomenon can be attributed to the fact that, when a higher SR is employed, more leaf nodes are created and the profiling algorithm functions in a more fine-grained manner. At this point, the exact structure of the leaf nodes (if they are oblique or flat) is not very important. However, when the algorithm must work with fewer leaves, i.e., lower sampling rates, the importance of the leaf shape becomes crucial, hence the performance boost the oblique cuts get.

A point that is not shown and stressed in the results so far is that oblique Decision Trees, apart from a minor per-

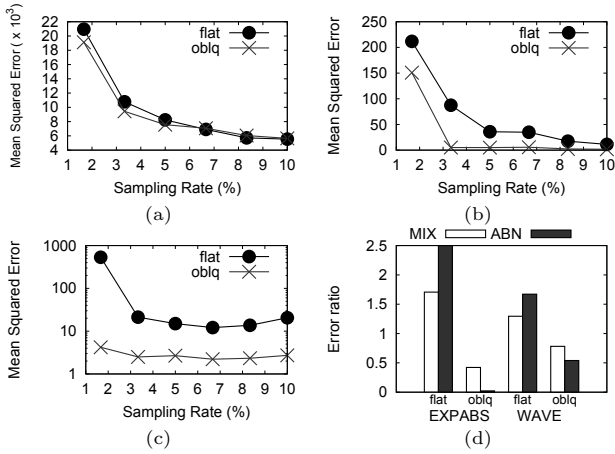


Figure 8: Accuracy vs flat and oblique cuts

formance boost, offer the ability to accurately approximate points of the performance function with patterns spanning to multiple dimensions of the Deployment Space. When measuring the accuracy of the model in the entire Deployment Space, as in Figure 8 (a), this can be overlooked but becomes apparent when focusing on the region containing the pattern. To showcase this, we conduct the following experiment: Assume function EXPABS of Table 2. This function is minimized when the exponent is equal to zero, hence  $a_1 \cdot x_1 \cdots a_n x_n = 0$ , and, along this line, the function is not differentiable. We again compare the flat and oblique approaches for a Deployment Space formed of two dimensions and 1600 points but now use two different test sets: (i) points from the entire Deployment Space (as before) and (ii) points that are relatively close to the pattern (the aforementioned line). Figure 8 (b) corresponds to the case where the test set is drawn from the entire Deployment space, while Figure 8 (c) to the case where only points close to the abnormality, i.e., points of the Deployment Space with distance less than  $\epsilon = 10^{-3}$  from the line are tested.

While the difference in (b) is considerable for the particular sampling rates (a gain of 30% to 90%), when testing against points close to the abnormality we observe that the oblique version manages to achieve error rates that are orders of magnitude lower (the vertical axis is in logarithmic scale) than those achieved with the flat Decision Trees. To further evaluate the impact of the test set into the measured accuracy for different performance functions, we repeat the previous experiment for EXPABS and WAVE (which also contain similar complex patterns) for a set sampling rate of 2%. We measure the accuracy of the model when the test points are picked from (a) the entire Deployment Space (ALL), (b) close to the “abnormal” region (ABN) and (c) both (MIX). For MIX, half of the test points are far from the abnormality and the other half is located in a distance less than  $\epsilon$ . Figure 8 (d) showcases the respective results. The produced errors for MIX and ABN are divided with the error of ALL for each execution (ALL is thus omitted since it is always equal to 1). Our results demonstrate that, for flat Decision Trees, the modeling error increases the more we focus on the abnormal patterns of the Deployment Space. On the other hand, oblique cuts produce much more accurate results, vastly reducing their induced errors as we focus on abnormality areas. Different profiling algorithms were also

tested around ABN; Our evaluation indicated that DTA was the only algorithm that achieved such an accuracy gain, as the other methodologies presented worse results around the abnormality region.

In summary, utilization of the oblique tree manages to identify the abnormality of the space; Even for very low SR, such patterns are adequately approximated. This means that oblique Decision Trees manage to reveal complex concepts of the performance function: Patterns that may represent before profiling; a discontinuity, i.e., a hyperplane that separates the performance function in different regions into which different behavior is exhibited (as in the EXPABS and WAVE cases); in general, any pattern that characterizes the structure of the performance function. This interesting quality is reflected into the structure of the tree itself, since the test nodes represent the boundaries of the space. Thus, apart from the general modeling functionality, the Decision Tree can also be useful for providing intuition relative to “interesting” regions of the performance function, and, consequently, it can be utilized as a tool for recognizing conditions that induce application bottlenecks, performance peaks, etc.

### 4.3.3 Cost-aware profiling

So far, we have assumed that all Deployment Space points are equivalent, in the sense that we have not examined the deployment configuration they represent: A point representing a deployment configuration of 8 VMs, each of which has 8 cores, is equivalent to a point representing 1 VM with 1 core. However, since the choice of a point results in its actual deployment, it is obvious that this choice implicitly includes a (monetary) cost dimension that has not been addressed. We now examine DTA’s ability to adapt when such a cost consideration exists. Let us define the following cost models:

- Bayes:  $|\text{nodes}| \times |\text{cores}|$
- Wordcount:  $|\text{nodes}| \times |\text{cores}|$
- Media Streaming:  $|\text{servers}|$
- MongoDB:  $|\text{MongoS}| + |\text{MongoD}|$

We have chosen realistic cost models, expressed as functions of the allocated resources (VMs and cores). Let us recall that Media Streaming and MongoDB utilize uncore VMs. Hence, their cost is only proportional to the number of allocated VMs.

We execute DTA using the Equation 1, presented in Section 3.3 where the error and size parameters positively influence the score of each leaf and cost is a negative factor. For  $w_{error} = 1.0$  and  $w_{cost} = 0.5$ , we alter the weight of the cost parameter between 0.2 and 1.0 for SR of 3% and 20%. We provide our findings in Table 5, in which we present the percentage difference in the profiling error (measured in MSE) and cost for each case, against the case of  $w_{cost} = 0.0$ .

For low sampling rates, increasing values for  $w_{cost}$  does not heavily influence the profiling cost. Specifically, for the MongoDB case, the cost reduces by a marginal factor (around 4% in the most extreme case) whereas the error increases by 13%. On the contrary, for high sampling rates, it becomes apparent that the consideration of the cost increases its impact as the application profiles are calculated even 26% less expensive than the case of  $w_{cost} = 0$ , e.g., in the Media Streaming case for  $w_{cost} = 1.0$ . Furthermore, it is obvious that for increasing  $w_{cost}$ , the cost becomes a more important factor for the leaf score and, hence, the cost

**Table 5: MSE and Cost for different cost weights**

App/tions	SR	MSE			Cost		
		0.2	0.5	1.0	0.2	0.5	1.0
Bayes	3%	+1%	-1%	-2%	-1%	-1%	-1%
	20%	+4%	+10%	+5%	-7%	-9%	-12%
Wordcount	3%	-1%	-5%	-1%	-4%	-6%	-1%
	20%	0%	+13%	+19%	-6%	-8%	-18%
Media Str.	3%	-1%	-3%	+3%	-1%	-5%	-6%
	20%	-6%	-2%	-8%	-7%	-11%	-26%
MongoDB	3%	+6%	+12%	+13%	-2%	-3%	-4%
	20%	-1%	-7%	-7%	-6%	-9%	-12%

degradation becomes more intense. Regarding the profiling accuracy, in most cases the error remains the same or its increase does not exceed 10%. A notable exception from this is the Wordcount case, where we can see that the MSE increases rapidly with increasing  $w_{cost}$  values and even reaches a growth of 19% in the case where  $w_{cost} = 1.0$ . From this analysis, we can conclude that cost-aware sampling becomes particularly effective for high sampling rates, which is also desirable since high sampling rates entail many deployments, i.e., increased cost. In such cases, the cost-aware algorithm has more room to improve the profiling cost whereas, on the same time, the accuracy sacrifice is totally dependent on the nature of the performance function; However, from our evaluation we can conclude that the accuracy degradation is analogous to the cost reduction, allowing the user to choose between higher accuracy or reduced deployment cost.

## 5. RELATED WORK

Cloud application performance modeling is a vividly researched area. The challenge of accurately predicting the performance of an application is hindered by the virtualization overhead inserted from the cloud software (hypervisors, virtual hardware, shared storage, etc.). To allow the problem decomposition, the proposed solutions are mainly focused on two directions: (a) modeling the performance of the cloud provider itself through cloud benchmarks, and (b) modeling the application performance in an infrastructure-agnostic way. The first approach is mainly focused on executing sets of typical cloud applications such as [6, 18, 26, 32] over different cloud providers and identifying the relationships between the cloud offerings and the respective application performance. Each benchmark is deployed over different clouds with different deployment configurations and the relation between the performance and the deployment setups is obtained. Industrial solutions such as [2, 3, 4] retain statistics and perform the analysis, providing comparisons between different public clouds, identification of the resources’ impact to the applications, etc. These results can then be generalized into custom user applications in order to predict their performance into different cloud providers.

Solutions based on the modeling of a specific cloud application can be further graded in three categories: (a) simulation based approaches, (b) emulation based approaches and (c) approaches involving the benchmarking of the application, i.e., the “black-box” approaches. In the first case, the approaches are based on known models of the cloud platforms [11] and enhance them with known performance models of cloud applications. CDOSim [19] is an approach that targets to model the Cloud Deployment Options (CDOs) and simulate the cost and performance for a cloud application. CloudAnalyst [50] is a similar work that simulates

large cloud applications and studies their performance for different cloud configurations. Finally, WebProphet [34] is a work that specializes in web applications. All the aforementioned works are based on the hypotheses that performance models regarding both the infrastructure and the application are known. On the contrary, our approach makes no assumptions neither for the application nor for the provider since it addresses both as black-boxes.

To bypass the assumption of a known performance model, emulation has been used. The idea is to deploy the application and capture performance usage traces for various scenarios. The traces are then “replayed” in the cloud to predict the application performance. CloudProphet [33] is an approach used for migrating an application into the cloud. It collects traces from the application running locally and replays them into the cloud, predicting the performance the application should achieve over the cloud infrastructure. //Trace [37] is another emulation based approach specializing in predicting the I/O behavior of a parallel application, identifying the causality between I/O patterns among different cluster nodes. In [25] a similar emulation approach is presented. The authors execute a set of benchmark applications in a cloud infrastructure measuring microarchitecture-independent characteristics and measure the relationship between a target application and the benchmarked application. According to this relationship, a performance prediction is extracted. Finally, in [38], a performance prediction approach is presented specialized in I/O-bound applications. Through microbenchmarking, the authors extract a performance model for the virtualized storage and apply this model to I/O intensive BigData applications, so as to predict their performance. All the aforementioned approaches tackle the problem of identifying either the application performance model or the infrastructure model, not both. Nevertheless, they can be viewed as less generic solutions than the one presented in this paper.

On the contrary, several approaches that make no assumptions regarding the application structure, have been suggested. Such approaches assume that the application is a black-box that receives a number of inputs (deployment configurations) and produces a number of outputs which correspond to application performance metrics. The application is deployed for some representative deployment configurations and performance metrics are obtained. The model is then constructed by utilizing statistical and machine learning techniques mapping the configuration space into the application performance. In [23, 14] a generic methodology is described used to infer the application performance of based on representative deployments of the configuration space. The approach tackles the problem of generalizing the performance for the entire deployment space, but does not tackle the problem of picking the most appropriate samples from the deployment space, as the suggested approach. PANIC [22] is a similar work, that addresses the problem of picking representative points during sampling. This approach favors the points that belong to the most steep regions of the Deployment Space, based on the idea that these regions characterize most appropriately the entire performance function. However it is too focused on the abnormalities of the Deployment Space and the proposed approach outperforms it. Similarly, the problem of picking representative samples of the Deployment Samples is also addressed by Active Learning [44]. This theoretical model introduces the term

of uncertainty for a classifier that, simply put, expresses its confidence to label a specific sample of the Deployment Space. Active Learning favors the regions of the Deployment Space that present the highest uncertainty and, as PANIC, fail to accurately approximate the performance function for the entire space, as also indicated by our experimental evaluation. Finally, in [30] and [31] two more generic black-box approaches are provided, utilizing different machine learning models for the approximation. Neither of these works, though, address the problem of picking the appropriate samples, since they are more focused on the modeling problem.

## 6. CONCLUSIONS

In this work, we revisited the problem of performance modeling for applications deployed over cloud infrastructures. Their configuration space can grow exponentially large, making multiple deployments for better profiling prohibitive. We proposed a methodology that utilizes Decision Trees to recursively partition and sample the Deployment Space, assuming a maximum number of cloud deployments constraint. Our approach manages to adaptively focus on areas where the model fails to accurately approximate application performance. We demonstrated that our method better approximates both real-life and synthetic performance functions with an accuracy that is adjustable to the deployment cost. Moreover, the utilization of oblique Decision Trees proved particularly effective at modeling application performance areas that are hard to approximate.

## 7. REFERENCES

- [1] Brightcove. <https://www.brightcove.com/en/>.
- [2] CloudHarmony. <https://cloudharmony.com/>.
- [3] CloudSpectator. <http://cloudspectator.com/>.
- [4] LoadImpact. <https://loadimpact.com/>.
- [5] Openstack Heat. <https://wiki.openstack.org/wiki/Heat>.
- [6] PerfKitBenchmark. <https://goo.gl/b4Xcij>.
- [7] Streambox. <http://www.streambox.com/streambox-cloud/>.
- [8] Wowza. <https://www.wowza.com/products/streaming-cloud>.
- [9] R. C. Barros, R. Cerri, P. A. Jaskowiak, and A. C. De Carvalho. A bottom-up oblique decision tree induction algorithm. In *Intelligent Systems Design and Applications (ISDA), 2011 11th International Conference on*, pages 450–456. IEEE, 2011.
- [10] L. Breiman, J. Friedman, C. J. Stone, and R. A. Olshen. *Classification and regression trees*. CRC press, 1984.
- [11] R. N. Calheiros, R. Ranjan, A. Beloglazov, C. A. De Rose, and R. Buyya. CloudSim: a toolkit for modeling and simulation of cloud computing environments and evaluation of resource provisioning algorithms. *Software: Practice and Experience*, 41(1):23–50, 2011.
- [12] B. J. Chee and C. Franklin Jr. *Cloud computing: technologies and strategies of the ubiquitous data center*. CRC Press, 2010.
- [13] B. F. Cooper, A. Silberstein, E. Tam, R. Ramakrishnan, and R. Sears. Benchmarking cloud serving systems with YCSB. In *Proceedings of the 1st ACM symposium on Cloud computing*, pages 143–154. ACM, 2010.
- [14] M. Cunha, N. Mendonça, and A. Sampaio. Cloud Crawler: a declarative performance evaluation environment for infrastructure-as-a-service clouds. *Concurrency and Computation: Practice and Experience*, 2016.
- [15] E. Dede, M. Govindaraju, D. Gunter, R. S. Canon, and L. Ramakrishnan. Performance evaluation of a mongodb and hadoop platform for scientific data analysis. In *Proceedings of the 4th ACM workshop on Scientific cloud computing*, pages 13–20. ACM, 2013.
- [16] T. G. Dietterich. Ensemble methods in machine learning. In *International workshop on multiple classifier systems*, pages 1–15. Springer, 2000.
- [17] C. Dismuke and R. Lindrooth. Ordinary least squares. *Methods and Designs for Outcomes Research*, 93:93–104, 2006.
- [18] M. Ferdman, A. Adileh, O. Kocberber, S. Volos, M. Alisafae, D. Jevdjic, C. Kaynak, A. D. Popescu, A. Ailamaki, and B. Falsafi. Clearing the clouds: a study of emerging scale-out workloads on modern hardware. In *Proceedings of the seventeenth international conference on Architectural Support for Programming Languages and Operating Systems, ASPLOS '12*, pages 37–48, New York, NY, USA, 2012. ACM.
- [19] F. Fittkau, S. Frey, and W. Hasselbring. CDOSim: Simulating cloud deployment options for software migration support. In *Maintenance and Evolution of Service-Oriented and Cloud-Based Systems (MESOCA), 2012 IEEE 6th International Workshop on the*, pages 37–46. IEEE, 2012.
- [20] A. Gandini, M. Gribaudo, W. J. Knottenbelt, R. Osman, and P. Piazzolla. Performance evaluation of nosql databases. In *Computer Performance Engineering*, pages 16–29. 2014.
- [21] S. Geisser. *Predictive inference*, volume 55. CRC press, 1993.
- [22] I. Giannakopoulos, D. Tsoumakos, N. Papailiou, and N. Koziris. PANIC: Modeling Application Performance over Virtualized Resources. In *Cloud Engineering (IC2E), 2015 IEEE International Conference on*, pages 213–218. IEEE, 2015.
- [23] M. Gonçalves, M. Cunha, N. C. Mendonca, and A. Sampaio. Performance Inference: A Novel Approach for Planning the Capacity of IaaS Cloud Applications. In *Cloud Computing (CLOUD), 2015 IEEE 8th International Conference on*, pages 813–820. IEEE, 2015.
- [24] M. Hall, E. Frank, G. Holmes, B. Pfahringer, P. Reutemann, and I. H. Witten. The WEKA data mining software: an update. *ACM SIGKDD explorations newsletter*, 11(1):10–18, 2009.
- [25] K. Hoste, A. Phansalkar, L. Eeckhout, A. Georges, L. K. John, and K. De Bosschere. Performance prediction based on inherent program similarity. In *Proceedings of the 15th international conference on Parallel architectures and compilation techniques*, pages 114–122. ACM, 2006.
- [26] S. Huang, J. Huang, J. Dai, T. Xie, and B. Huang. The hibench benchmark suite: Characterization of the

- mapreduce-based data analysis. In *New Frontiers in Information and Software as Services*, pages 209–228. Springer, 2011.
- [27] L. Hyafil and R. L. Rivest. Constructing optimal binary decision trees is NP-complete. *Information Processing Letters*, 5(1):15–17, 1976.
- [28] N. H. Kapadia, J. A. Fortes, and C. E. Brodley. Predictive application-performance modeling in a computational grid environment. In *High Performance Distributed Computing, 1999. Proceedings. The Eighth International Symposium on*, pages 47–54. IEEE, 1999.
- [29] D. J. Kerbyson, H. J. Alme, A. Hoisie, F. Petrini, H. J. Wasserman, and M. Gittings. Predictive performance and scalability modeling of a large-scale application. In *Proceedings of the 2001 ACM/IEEE conference on Supercomputing*, pages 37–37. ACM, 2001.
- [30] S. Kundu, R. Rangaswami, K. Dutta, and M. Zhao. Application performance modeling in a virtualized environment. In *High Performance Computer Architecture (HPCA), 2010 IEEE 16th International Symposium on*, pages 1–10. IEEE, 2010.
- [31] S. Kundu, R. Rangaswami, A. Gulati, M. Zhao, and K. Dutta. Modeling virtualized applications using machine learning techniques. In *ACM SIGPLAN Notices*, volume 47, pages 3–14. ACM, 2012.
- [32] A. Li, X. Yang, S. Kandula, and M. Zhang. CloudCmp: comparing public cloud providers. In *Proceedings of the 10th ACM SIGCOMM conference on Internet measurement*, pages 1–14. ACM, 2010.
- [33] A. Li, X. Zong, S. Kandula, X. Yang, and M. Zhang. CloudProphet: towards application performance prediction in cloud. In *ACM SIGCOMM Computer Communication Review*, volume 41, pages 426–427. ACM, 2011.
- [34] Z. Li, M. Zhang, Z. Zhu, Y. Chen, A. G. Greenberg, and Y.-M. Wang. WebProphet: Automating Performance Prediction for Web Services. In *NSDI*, volume 10, pages 143–158, 2010.
- [35] S. Marston, Z. Li, S. Bandyopadhyay, J. Zhang, and A. Ghalsasi. Cloud computing - The business perspective. *Decision support systems*, 51(1):176–189, 2011.
- [36] M. D. McKay, R. J. Beckman, and W. J. Conover. A comparison of three methods for selecting values of input variables in the analysis of output from a computer code. *Technometrics*, 42(1):55–61, 2000.
- [37] M. P. Mesnier, M. Wachs, R. R. Simbasivan, J. Lopez, J. Hendricks, G. R. Ganger, and D. R. O’hallaron. //Trace: parallel trace replay with approximate causal events. USENIX, 2007.
- [38] I. Mytilinis, D. Tsoumakos, V. Kantere, A. Nanos, and N. Koziris. I/O Performance Modeling for Big Data Applications over Cloud Infrastructures. In *Cloud Engineering (IC2E), 2015 IEEE International Conference on*, pages 201–206. IEEE, 2015.
- [39] J. Quinlan. C4. 5: Program for Machine Learning Morgan Kaufmann. *San Mateo, CA, USA*, 1993.
- [40] J. R. Quinlan. Induction of decision trees. *Machine learning*, 1(1):81–106, 1986.
- [41] J. R. Quinlan. Bagging, boosting, and c4. 5. In *AAAI/IAAI, Vol. 1*, pages 725–730, 1996.
- [42] L. Rokach. Ensemble-based classifiers. *Artificial Intelligence Review*, 33(1-2):1–39, 2010.
- [43] F. Rosenblatt. Principles of neurodynamics. perceptrons and the theory of brain mechanisms. Technical report, DTIC Document, 1961.
- [44] B. Settles. Active learning literature survey. *University of Wisconsin, Madison*, 52(55-66):11, 2010.
- [45] C. Stewart and K. Shen. Performance modeling and system management for multi-component online services. In *Proceedings of the 2nd conference on Symposium on Networked Systems Design & Implementation-Volume 2*, pages 71–84. USENIX Association, 2005.
- [46] R. S. Sutton and A. G. Barto. *Reinforcement learning: An introduction*. MIT press, 1998.
- [47] Y. Tao and M. T. Özsu. Efficient decision tree construction for mining time-varying data streams. In *Proceedings of the 2009 Conference of the Center for Advanced Studies on Collaborative Research*, pages 43–57. IBM Corp., 2009.
- [48] S. Vadera. Csnl: A cost-sensitive non-linear decision tree algorithm. *ACM Transactions on Knowledge Discovery from Data (TKDD)*, 4(2):6, 2010.
- [49] V. K. Vavilapalli, A. C. Murthy, C. Douglas, S. Agarwal, M. Konar, R. Evans, T. Graves, J. Lowe, H. Shah, S. Seth, et al. Apache Hadoop YARN: Yet Another Resource Negotiator. In *Proceedings of the 4th annual Symposium on Cloud Computing*, page 5. ACM, 2013.
- [50] B. Wickremasinghe, R. N. Calheiros, and R. Buyya. Cloudanalyst: A cloudsims-based visual modeller for analysing cloud computing environments and applications. In *Advanced Information Networking and Applications (AINA), 2010 24th IEEE International Conference on*. IEEE, 2010.

## APPENDIX

### A. SYSTEM OVERVIEW

As showcased in Algorithm 1, application profiling entails: (a) The sampling of the Deployment Space, (b) the Deployment of the chosen samples and (c) the construction of the end model. So far, we have focused our analysis and evaluation on the theoretical aspects of the methodology, ignoring the engineering part that entails the automatic deployment of the application, the enforcement of different resource- and application-level configuration parameters and the retrieval of the performance metric. Although these aspects are orthogonal to our methodology, in the sense that different cloud infrastructures, solutions and software can be utilized without altering the proposed profiling algorithm, the utilized solutions can have a great impact in the profiling time and the level of automation. In this section, we provide a brief overview of the tools utilized to create a fully-automated application profile.

Our implementation was based on Openstack and its deployment tool, Heat [5]. Heat is responsible for the deployment and the orchestration of virtual resources, including Virtual Machines, virtual networks, ports, block devices, volumes, etc. An application description, referred to as a Heat Orchestration Template (*HOT*), is, essentially, the blueprint of the application, describing its architecture and

main components and supports a set of parameters that can be defined during its instantiation. This way, Heat decouples the static application information, e.g., its architecture, from the dynamic information that must be provided in runtime, e.g., the flavors of the different VMs, application level parameters, etc.

When a new application deployment is spawned, Heat first allocates the necessary resources, in the correct order. For example, if a VM depends on a volume, the VM allocation starts upon the volume creation. After all the VMs are launched, Heat executes user-specified scripts, included in the HOT, in order to orchestrate the resources. Furthermore, to ease the application configuration, Heat also supports parameterized script execution that enables the scripts to be executed with different parameters and ensure that different resources are properly utilized. For example, the number of cores or the amount of RAM of a VM can be provided as a parameter during the HOT instantiation and, according to the value of this parameter, the script can set the appropriate parameter in the application’s configuration file. Through this powerful mechanism, the problem of describing a complex application is reduced into creating a parameterized Heat template that can be launched according to user-defined parameters.

In our case, we created four HOTs for each application of Table 1 and mapped each Deployment Space dimension into a unique HOT parameter (per application). This way, the deployment of a single Deployment Space point entails the deployment of the respective HOT with the appropriate parameters that reflect the aforementioned point. The workload-specific parameters are addressed in a unified way, as HOT parameters can also be visible to the user-specified scripts. When the workload finishes, the performance metrics are inserted into a centralized database and processed in order to resume the profiling algorithm execution. To reduce the deployment time, we have constructed precooked VM images (based on Ubuntu x64 14.04 images) that contain the necessary software. This way, the deployment only entailed the resource allocation, VM bootstrapping and workload execution.

In our experimental platform, the average VM creation time is around  $60 \pm 20$  sec and the average VM bootstrap time is  $30 \pm 10$  sec. Both times are measured to be independent of the VM flavor, i.e., the amount of cores, RAM and disk utilized by the VM. The workload execution time greatly varies among different applications and, in our case, dominates the entire deployment time. For each application, we estimate the average execution time along with the respective standard deviation and present them in Table 6.

**Table 6: Workload execution times (sec)**

Application	Average Time	Std. Deviation
Bayes	250	250
Wordcount	270	250
Media Streaming	350	350
MongoDB	150	130

It must be noted that our approach is capable of parallelizing the deployment of different samples: When the expansion of the Decision Tree in a specified step is finished, the samples that have been chosen can be deployed in-parallel. We recall here that the amount of samples chosen at each

algorithm step is determined by  $b$ , as described in Section 3. When  $b$  becomes equal to  $B$ , that corresponds to the maximum number of cloud deployments executed by our algorithm, our approach degenerates into a Random Sampler and the highest parallelization is achieved, although accuracy is sacrificed, as shown in Section 4.3.1. Taking into consideration this comment and based on the average Deployment and Workload execution times, we can roughly estimate the average time needed for the estimation of a profile for application  $A$ , as a function of  $B$  and  $b$  as follows:

$$ProfilingTime(B, b, A) = \left\lceil \frac{B}{b} \right\rceil \times (T_{creation} + T_{boot} + T_w(A))$$

where  $T_{creation}$  refers to the VM creation time,  $T_{boot}$  refers to the VM boot time and  $T_w$  is the workload execution time for application  $A$ .

## B. APPLICATION ANALYSIS

In this section we provide a thorough analysis of the applications utilized throughout the experimental evaluation, in Section 4. We choose to demonstrate our profiling methodology over applications with diverse characteristics covering both *batch* and *online* functionality. Bayes and Wordcount are typical examples of the former category, while Media Streaming and MongoDB are representative online ones. We choose two batch applications implemented in two different systems (Spark and Hadoop respectively) in order to cover both in-memory and disk-based computations respectively. Regarding the online applications, Media Streaming was chosen for two reasons: First, media/video streaming applications are very popular and tend to become an excellent use case for cloud computing [8, 7, 1], especially due to its decentralized and on-demand resource allocation nature. Second, its architecture, consisting of a storage backend and a set of horizontally scalable Web Servers, is very popular among cloud applications [12]. Finally, MongoDB is a popular document store, widely used as a database backend among various applications. In all cases, we opt for representative use cases of applications deployed over cloud infrastructures. Nevertheless, we emphasize that both the nature and the behavior of the selected application is orthogonal to our approach, as the proposed methodology successfully models applications of varying diversity.

**Table 7: Application complexity and correlations**

Application	$R^2$	Dimension	$r$
<b>Bayes</b> (execution time)	0.56	YARN nodes	-0.24
		# cores/node	-0.34
		memory/node	-0.49
		# of documents	0.51
<b>Wordcount</b> (execution time)	0.57	# of classes	0.00
		YARN nodes	-0.44
		# cores/node	-0.20
		memory/node	-0.38
<b>Media Streaming</b> (throughput)	0.46	dataset size	0.49
		# of servers	0.46
		video quality	-0.41
<b>MongoDB</b> (throughput)	0.55	request rate	0.28
		# of MongoD	0.33
		# of MongoS	0.50
		request rate	0.44

In order to provide more information regarding the behavior of the chosen applications, we first evaluate the nature of the performance functions and compare them to a linear function with the methodology described in Section 4: Using *all* the available performance points, we construct a linear model that best fits the data (with Ordinary Least Squares) and, then, compare this model to the original data points using  $R^2$ . In Table 7 we provide our findings. According to the categorization provided in Table 2 and based on the applications' scores, we observe that all the tested applications belong in the AVERAGE category and are quite different from their linear equivalent functions.

The selected dimensions for each application were chosen in order to reflect an actual profiling scenario, in which the application dimensions can vary in importance. To quantify this importance, we measure the correlation between the input and output dimensions using Pearson correlation coefficient  $r$ , as demonstrated in Table 7; The output dimensions are listed beneath the application names. A negative sign indicates that the growth of one dimension has a negative impact on the output dimension. For example, when increasing the number of YARN nodes in Bayes, the execution time of the job decreases. Values close to zero indicate that the specified dimensions are of low importance. For example, in Bayes, the number of classes used for the classification does not affect the execution time of a job. It is important for a profiling methodology to be able to efficiently handle dimensions that are, eventually, proven to be of low importance, since it is quite possible that when a new application is submitted for profiling, the user cannot be aware of which dimensions have a greater impact on the application performance. Such input dimensions increase the dimensionality of the Deployment Space, without adding any extra information. Our scheme manages to efficiently handle these dimensions due to the utilization of Decision Trees: The multidimensional cuts, created during the sampling phase, ignore the least important dimensions and focus on splitting the performance function based on the more important variables, increasing this way the profiling accuracy.

## C. EXTENDED EVALUATION

### C.1 MAE for varying Sampling Rate

Figure 9 describes the accuracy of the proposed methodology against UNI, PANIC and ACTL for varying Sampling Rates, measured in terms of MAE.

Comparing Figure 9 with Figure 6, it is apparent that both MSE and MAE provide a similar picture between the different profiling methodologies as DTA outperforms its competitors in all cases, UNI seems to present the next best results and PANIC and ACTL present the worst accuracy, due to their aggressive exploitation policy that focuses on the abnormalities of the Deployment Space. Specifically, DTA produces results even 3.5 times better than the next best algorithm (for MongoDB,  $SR = 6\%$ ) and the gap between the profiling methodologies increases with increasing  $SR$  for all cases, but for the Media Streaming case, where UNI achieves the same accuracy level.

### C.2 Optimizations

We evaluate the impact of the optimization presented in Section 3.4, i.e., the construction (from scratch) of the Decision Tree, so as to correct erroneous cuts of the Deployment

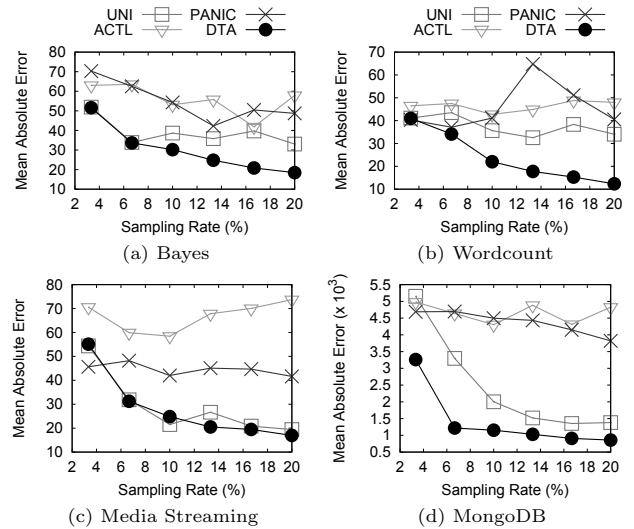


Figure 9: Accuracy vs sampling rate (MAE)

Space during the initial algorithm iterations. In Figure 10, we provide results for varying  $\frac{B}{b}$ ,  $SR = 10\%$  for the case of Bayes. The *online* training scheme represents the incremental expansion of the Decision Tree at each iteration whereas the *offline* training scheme refers to the case of reconstructing the tree at each iteration.

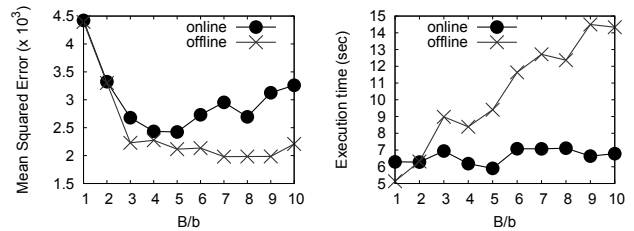


Figure 10: Accuracy vs training type

When  $b$  receives relatively high values (compared to  $B$ ), the impact of offline training is marginal to the performance function. While  $\frac{B}{b}$  increases, the impact of offline training increases, since the profiling algorithm produces models with lower error. This behavior is reasonable, since small values of  $b$  lead to more algorithm iterations, meaning that the cuts made on the initial steps of the algorithm were decided based on a very small portion of the samples. This leads to the conclusion that offline training boosts the algorithm's accuracy when  $\frac{B}{b}$  receives high values or, equivalently,  $b$  is minimized. In terms of execution time, since offline training entails the total reconstruction of the Decision Tree, the algorithm needs considerably more time to terminate, as demonstrated by the right plot in Figure 10. However, since the time needed to deploy and orchestrate the application is considerably larger, an overhead in the order of a few seconds is marginal.

### C.3 Partitioning

As presented in Section 3.2, a leaf node is separated by a boundary line in such a way that the samples of the different groups best fit into linear models. In this Section, this partitioning mechanism is compared to the most popular

Variance Reduction methodology, that targets to minimize the intra-group variance of the target dimension. In Figure 11, we provide DTA's error and execution time for the two different partitioning techniques, for different  $\frac{B}{b}$ ,  $SR = 5\%$  for the Bayes application.

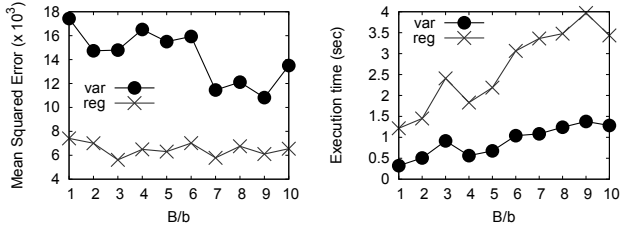


**Figure 11: Accuracy vs partitioner type**

From Figure 11, it becomes apparent that the Variance metric fails to partition the leaves as accurately as the regression methodology. Specifically, the regression technique achieves MSEs of 1.5 – 2.5 times lower than of the variance technique. The extra computation cost increases the execution time of the algorithm from 1.5 to 4 seconds, a difference which is marginal to the deployment cost of the application. We have to note here that the rest of the homogeneity heuristics, such as GINI impurity, Information Gain, etc., were not considered since they are only used for classification.